Original Article

Anterior Cruciate Ligament Tear Detection In Mri Images Using Multi-Neighbor Local Binary Pattern

[1]Kavita Joshi, [2]Dr. K. Suganthi

[1]Research Scholar, VIT Chennai, India
[1]Asst.Prof., Dr. D. Y. Patil Institute of Engineering Management and Research, Akurdi Pune
Corresponding Author: [2]Assistant Professor (Sr.), VIT Chennai, India.
[2]suganthi.k@vit.ac.in, [1]kavitap.joshi2018@vitstudent.ac.in
DOI: 10.47750/pnr.2022.13.S07.895

Abstract

Knee ligament injuries are very common in sportspersons playing football, volleyball, basketball, tennis, etc. Anterior Cruciate Ligament (ACL) tear occurs frequently due to extra stretching and sudden movement that causes extreme pain to the patient. There is a need for an accurate, efficient, and robust computer aided system for ACL tear detection. In this paper, we present multi-directional Multi-neighbor Local binary pattern (MNLBP) texture descriptor for the ACL tear detection knee magnetic resonance images (MRI). Performance of MNLBP is evaluated using K-nearest neighbor (KNN) and Support Vector Machine Classifiers. Performance of the proposed system is evaluated on the MRNet knee MRI dataset based on sensitivity, specificity, and accuracy. The proposed MNLBP outperformed the traditional LBP and resulted in sensitivity of 0.87 and 0.88; specificity of 0.92 and 0.92; and accuracy of 88.92% and 89.41% for the KNN and SVM classifiers.

Keywords: Multi-Neighbor Local Binary Pattern, Anterior Cruciate Ligament, K-nearest neighbor, Support Vector Machine

I. INTRODUCTION

The knee is the largest joint in the human body that carries the body weight, helps for movement in the vertical and horizontal directions such as jumping, walking, running, etc [1][2]. It joins the leg bone (tibia and fibula) with thigh bone (femur) as well as knee cap (patella) with femur using four major ligaments such as anterior cruciate ligament (ACL), Posterior cruciate ligament (PCL), Medial collateral ligament (MCL) and Lateral collateral ligament (LCL) [3]. ACL is situated at the central position of the knee that controls the forward movement and rotation of the Tibia whereas posterior cruciate ligament (PCL) is located in the back of the knee that controls backward movement of the tibia. MCL and lateral LCL give strength to the inner knee and outer knee respectively, act as shock absorber and distribute the weight evenly with each turn or shape. The structure of knee anatomy is shown in Fig. 1 [4][5].

ACL tear is most common injured ligament due to extra stretching and sudden twisting motion due to accident or sports like football, basketball, skiing, volleyball, tennis, etc. Around 76% of knee tear injuries are related to ACL tear [6][7][8]. ACL tear can be diagnosed using diagnosis using X-ray, Computer Tomography (CT scan), Ultrasound, MRI, Arthroscopy or radiological method are used [9][10]. But MRI images are often selected because of higher resolution, multi-planar slice capability, superior signal to noise ratio (SNR) and absence of ionizing radiation [11].

The current standard for diagnosis of sports medicine knee injuries based on imaging is the use of magnetic resonance imaging (MRI) for anterior cruciate ligament (ACL) and meniscus tears. However, a number of factors might reduce

the diagnostic efficacy of MRI, including: (1) minor partial or full rips, (2) observer bias and inexperience, (3) imaging artifacts, (4) the existence of concurrent injuries, and (5) inadequate MRI studies. By easing clinical decision-making and enhancing patient care, the use of AI techniques may overcome these problems. As a result, the present study's objectives were to (1) that effectiveness with that of human clinical specialists and (2) assess the diagnostic effectiveness of AI approaches for identifying ACL and meniscus injuries. The authors postulated that AI approach performance would be superior to human examiners for the identification of ACL and meniscus injuries [8-11].

Manual diagnosis of the knee ligament tear detection is wearisome, time consuming and unpredictable due to complex structure of the medical images. Hence, to cope up such issues computer aided diagnosis is introduced for analysis of ACL tears using various artificial intelligence based methods [12].

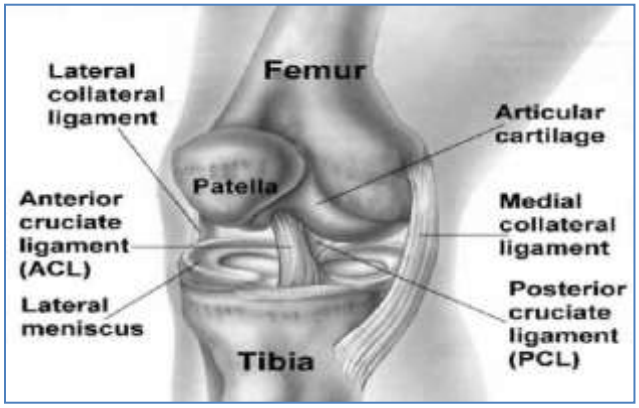

Fig. 1 Leg knee anatomy [4]

Štajduhar et al. [13] presented semi-automatic ACL rupture detection using Histogram of oriented gradients (HOG) and GIST features. They have used support vector machine (SVM) and random forest classifier that can detect partial and complete rupture of knee ligament in MRI images. Piotr et al. [14] investigated watershed algorithm for the segmentation and detection of knee joint injuries using MRI images. It has given 83.3% correct diagnosis of meniscal tear on 7 MRI images (3 normal, 4 injured). Piotr Zarychta et al. [15] proposed fuzzy c-mean algorithm for the segmentation of ACL and PCL from leg MRI images that and they mentioned that it can help in ACL and PCL tear detection. Mazlan et al. [16] suggested Active contour model (ACM) and radial basis SVM (RBF-SVM) for the classification of normal, partial injury and crucial injury using knee X-ray image. Bien et al. [17] implemented deep convolutional neural network (DCNN) for ACL that resulted in an accuracy of 95% for ACL and meniscal tear detection. Later, Lai et al. [18] designed high level features using deep CNN and traditional feature set to deal with the problem of high resolution and low dataset. It has given 90.2% and 90.15% accuracy for ISIC2017 and HIS2828 dataset respectively. Subsequently, Liu et al. [19] proposed two deep CNN layers to segment the ACL from the T2 weighted MRI knee images for the detection of the structural abnormalities. The area under the ROC curve for the ACL tear detection of system was 0.98. Consequently, Recurrent CNN (R-CNN) [20] has been used for segmentation and detection meniscus region. The performance of the system depends upon the segmentation of ACL using morphological filter and over-segmentation or under-segmentation may leads to the poor performance. Recently, deep learning models based on CNN have been successfully presented for knee injuries detection [21][22].

Very less work has been presented for the ACL tear detection using larger MRI database. Various deep learning based systems have been incorporated provide poor results for smaller dataset, needs huge number of trainable parameters, complex architecture of model, and infeasibility to implement on the standalone device because of computational burden. The Traditional texture based features arerarely used for the ACL tear detection. Therefore, it is important to analyze the textural properties of the ACL MRI images.

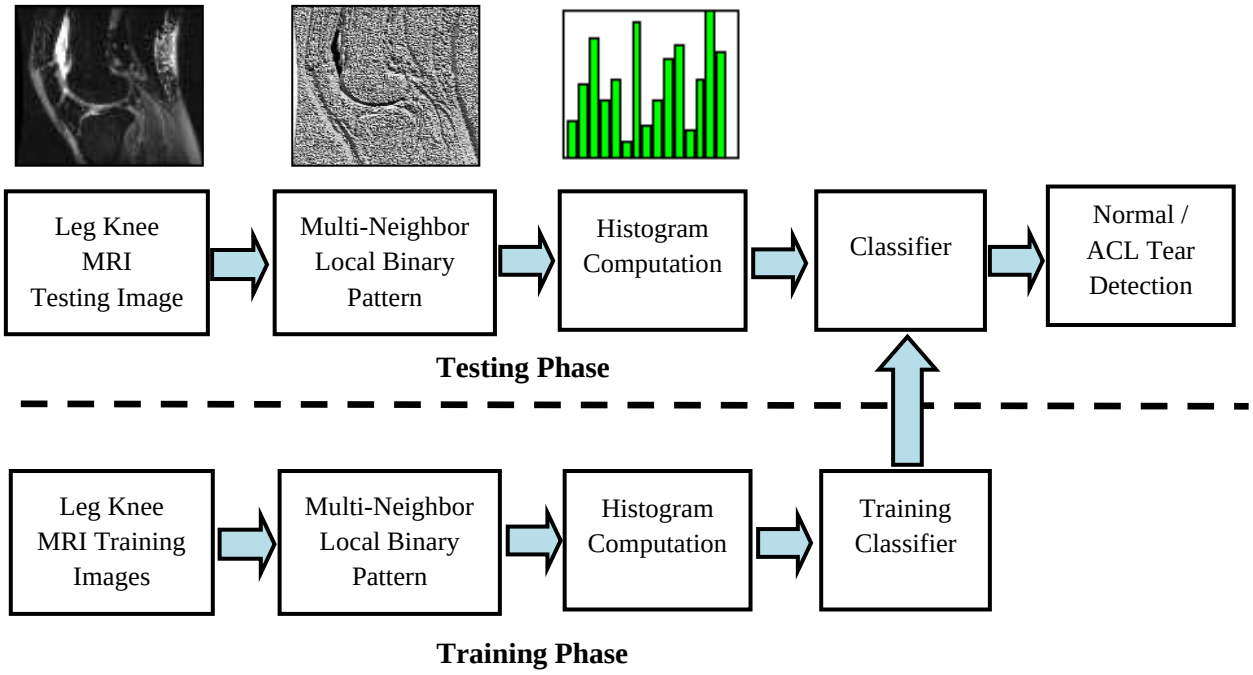

Fig. 2 Flow diagram of proposed system

In this paper, we proposed multidirectional multi-neighbor local binary pattern (MNLBP) for the Anterior Cruciate Ligament tear detection in knee MRI images. Histogram of MNLBP descriptor is used as feature vector. Performance of the proposed algorithm is evaluated on the Leg knee MRI images from MRNet dataset using K-Nearest Neighbor (KNN) and linear Support Vector Machine classifier (SVM). The flow diagram of proposed system is shown in Fig. 2.

This paper is organized as follow: section II gives the brief information of traditional LBP and its variants. Section III describes the proposed methodology in details. Experimental results and discussions are provided in section IV. Finally, section V concludes the paper and gives the future scope of the work.

II. Traditional Local Binary pattern and it's variants

Local binary pattern (LBP) is texture descriptor which describes the local texture of gray scale image [23]. It has attracted researchers' attention due to its simplicity and discriminative power for various image processing applications such as face recognition, medical image processing, bio-metrics, content based image retrieval, activity analysis, etc [24]. It is robust against monotonic gray scale changes, illumination changes, blur and shadow.

In the traditional LBP, center value is selected for the thresholding if the neighboring pixel value is greater than center pixel then it is considered as binary one otherwise considered as zero. The binary pattern is then converted in to equivalent decimal value as given in equation 1 and 2 [25].

$$\mathrm{LBP}\,(C_x, C_y) = \sum_{p=0}^{7} S(g_p - g_c).\,2^p \quad (1)$$

$$S(x) = \begin{cases} 0, & x < 0 \\ 1, & x \geq 0 \end{cases} \quad (2)$$

Where g_p represents gray intensity value of neighboring pixels of center pixel in local window, g_c is the gray intensity of the center pixel (C_x, C_y).The process of traditional LBP is shown in Fig. 3.

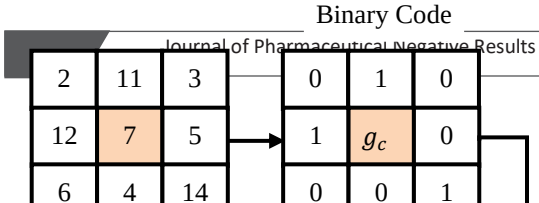

Fig. 3 Traditional LBP process

In past,modifications of LBP has been presented to improve the robustness of the algorithm. In the multi-scale LBP (MLBP) [26], LBP operator is extended for multiple radius and histograms are concatenated for different radii. It is observed that few LBP pattern occurs frequently such as curves, edges, line ends, spots and flat areas. Zhao and Pietikäinen [27] investigated volume LBP (VLBP) [5] for motion analysis in dynamic textures. It considered co-occurrences of LBP in three dimensions using circular neighborhood. Hafiane et al. [28] proposed median binary pattern (MBP) that considered median value for the thresholding the local pixel values. Tan and Triggs [29] invented three level local ternary pattern (LTP) to describe the texture at uniform regions of image. In this centered value is used for thresholding and three levels are encoded (1,0 and -1). The LTP pattern is then divided into two binary patterns by considering positive and negative values. Further, Guo et al. [30] presented completed LBP (CLBP) that decomposed the local texture differences in signs and magnitudes to measure the contrast of LBP. It included texture information and information related to intensity representation. Next, center-symmetric LBP (CS-LBP) [31] has been proposed to minimize the feature vector length of the original LBP. It compares only center symmetric pixels with center pixel thus resulted in feature vector length of 16 compared to 256 of original LBP. Zhang et al. [32] proposed higher-order local derivative patterns (LDPs) for face recognition that provided more detailed information about texture. The performance of LDP was limited due to higher feature vector length, rotation variation and sensitivity to noise compared to original LBP.In Transition Local Binary Patterns (t-LBP) [33], all neighboring pixels are compared in clockwise direction except the center pixel to represent the relation between neighboring pixels.To deal with rotation variation, Guo et al. [34] presented a rotation invariant local directional derivative pattern (LDDPs) that gives better rotation invariance. Hussain and Triggs[35] presented local quantized patterns (LQPs) that used vector quantization to represent the larger and deeper pattern. Orjuela et al. [36] presented geometric local textural patterns (GLTPs) as an extension of LBP that described the intensity variation on oriented neighborhood to describe the particular geometry around the center pixel. Further in [37] and [38], fuzzy based LBP are presented that considered fuzzy model for the thresholding. Addition of fuzzy membership increases the computation time and complexity of the algorithm. Over-Complete Local Binary Patterns (OCLBP) [39] considered overlapping of adjacent blocks that gives robust description of the local texture but resulted in larger feature vector length.Variants of LBP can describe the can extracts circular isotropic micro structure of the texture at single level which is insufficient to describe the complex texture. To deal with this issue Ding et al. [40] presented dual cross pattern (DCP) that computes the holistic and component level features. Though DCP has given better performance under various geometric variations it does not carry information about reference pixel and loses information regarding magnitude of difference [41].

Most of past LBP variants have focused on improvement of LBP performance by optimizing pre-processing before LBP, encoding, thresholding and LBP neighbors. Still performance of LBP is limited because of view and scale variation problem due to occlusion of image objects, less robustness to lighting variations, less spatiotemporal information

III. Proposed Multi-Neighbor Local Binary Pattern (MNLBP)

The proposed multidirectional multi-neighbor local binary pattern (MNLBP) considers the relation of reference pixel at multiple levels to describe the local region texture for the ACL tear detection in knee MRI images. Tear in ACL ligament disturbs the homogeneity of the knee MRI image that brings the changes in texture of image. It also captures the smooth changes over the MRI image texture. MNLBP computes the difference between neighboring pixel at various radii and center pixel in eight directions as shown in Fig. 4. The pixels nearer to the reference pixels are given more significance than the pixel far from reference pixel.

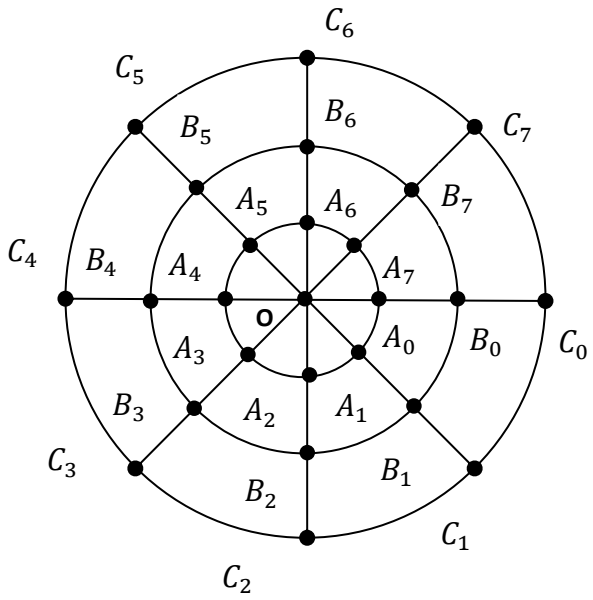

Fig. 4 Local sampling of MNLBP

Total 24 points are sampled around the centered pixel O. The level one sample points ($A_0\ to\ A_7$) are evenly located on the circle of radiusR_1,level two sample points ($B_0\ to\ B_7$) are evenly located on the circle of radius R_2 (level 2) while level three sample points ($C_0\ to\ C_7$) are evenly located on the circle of radius R_3 (level 3). The MNLBP descriptor computation is given by equation 3 and 4.

$$MNLBP\ (C_x, C_y) = \sum_{i=0}^{7} S((A_i - g_c) \times R_3 + (B_i - g_c) \times R_2 + (C_i - g_c) \times R_1)).\, 2^i \quad (3)$$

$$S(y) = \begin{cases} 0, & y < 0 \\ 1, & y \geq 0 \end{cases} \quad (4)$$

Fig. 5 shows LBP and MLBP texture descriptor for sagittal knee MRI image. MNLBP can better represent the smooth edges and the geometrical variations of the texture. After computation of MNLBP descriptor, histogram of single block is selected as feature vector having length of 256 as shown in the Fig. 6.Tear in ACL causes disturbances in the

homogeneity of the knee MRU textures which shows considerable variation in the MNLBP histogram compared to normal knee MRI.

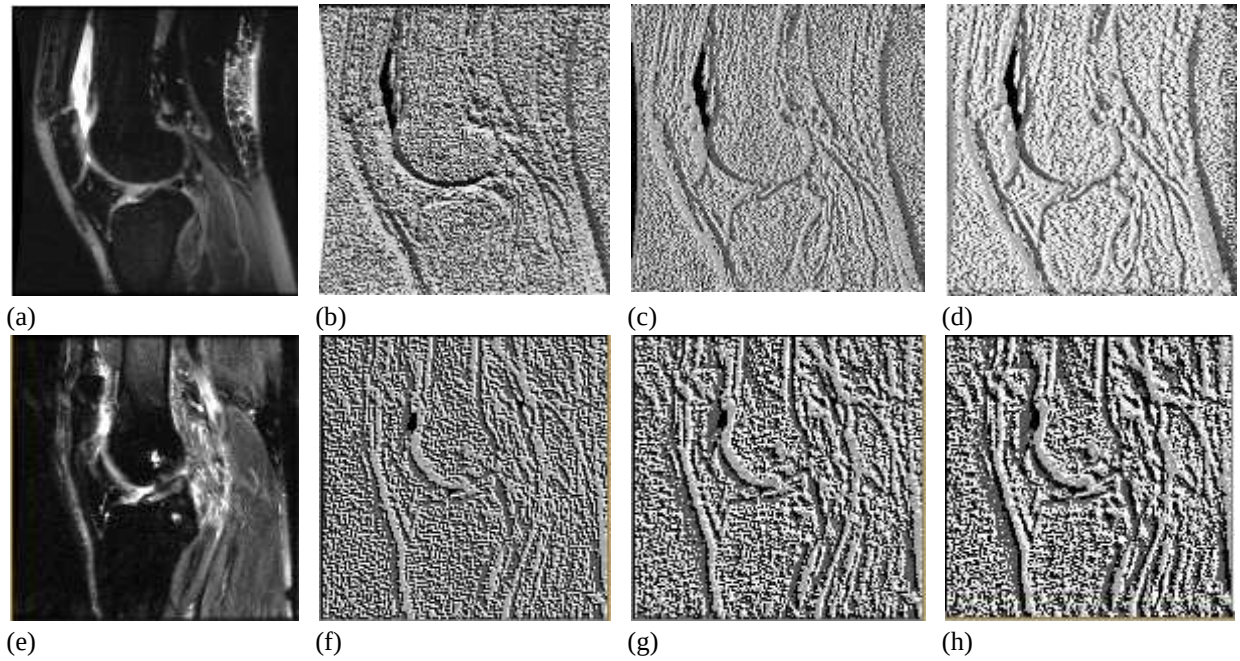

Fig. 5 a) Original Normal Knee MRI image b) LBP descriptor of normal image c) MNLBP descriptor (R=2) of normal image d) MNLBP descriptor (R=3) of normal image e) Knee MRI with ACL tear f) LBP descriptor of ACL tear g) MNLBP descriptor (R=2) of ACL tear h) MNLBP descriptor (R=3) of ACL tear

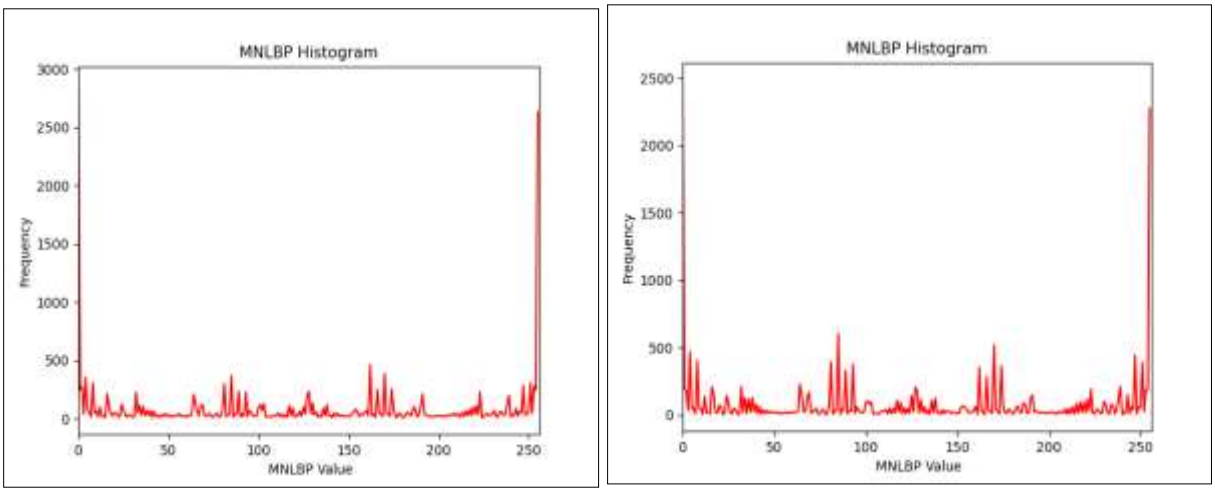

Fig. 6 Histogram for normal and ACL tear knee MRI radiographs (R=3)

For the classification of normal and ACL tear, KNN and SVM classifiers are used. Initially KNN is applied because of simplicity and lesser training time [42]. Euclidean distance is used as the distance metrics for matching purpose in KNN. For K=3 neighbors proposed system resulted in minimum error (see Fig. 7) and hence it is used for testing.

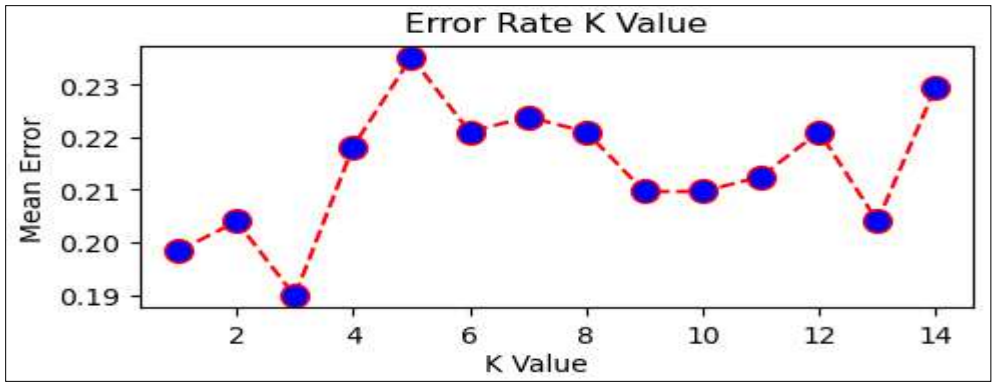

Fig. 7 Error rate for different K values for KNN classifier

Further, performance of the proposed texture feature extraction method is evaluated using SVM classifier. SVM has ability to deal with large dimensional features. We have used linear kernel function to generated hyperplane that separates the normal and ACL tear features. The features nearer to hyperplane are called as support vectors. It reduces the recognition time by comparing the testing samples with the support vectors [43].

The hyperplane is the function of the line for the input vector x = (x1, x2, x3,……,xn) with bias value (b) and weight (w) can be given in equation 5.

$$w.x + b = 0 \qquad (5)$$

The hypothesis function h is given by equation 6 which indicates that the points above the hyperplane are classified as normal (class +1) and points below the hyperplane are classified as ACL tear (class -1).

$$h(x_i) = \begin{cases} +1 & if wx + b \geq 0 \\ -1 & if wx + b < 0 \end{cases} \qquad (6)$$

Main aim of SVM is to maximize the margin that is a space between two lines of both classes. It can be calculated at the perpendicular distance between support vectors and hyper-plane [44].

The perpendicular distances of the hyperplane$W.X_i - b = 0$ to X_i (-1) and X_i (+1) can be given by equation 7 and 8.

$$d(-) = \frac{|W.Xi(-1) - b|}{\|b\|} = \frac{1}{\|b\|} \qquad (7)$$

$$d(+) = \frac{|W.Xi(+1) - b|}{\|b\|} = \frac{1}{\|b\|} \qquad (8)$$

SVM kernel converts the low dimensional feature data into higher dimensional feature data by adding extra dimensions to it. In the proposed system, a linear kernel is used that uses dot products between two samples as given in equation 9 [45].

$$K(x, y) = \phi(x).\phi(y) \qquad (9)$$

IV. EXPERIMENTAL RESULTS AND DISCUSSION

The proposed algorithm is implemented using Python-OpenCV programming on the personal computer having core i3 processor with speed of 2.64GHz, 4GB RAM and windows environment.

4.1 Dataset

Performance of the MNLBP is evaluated on MRNet knee joint MRI dataset [46]. MRNet dataset consists of MRI images in sagittal T2, coronal T1 and axial PD view with multiple frames that consists of ACL and meniscal tear. We have selected specific frames from the dataset in sagittal T2 view that consists of complete view of normal and tear ligament. Each image in dataset is having dimension of 256×256 pixels. We have selected 845 normal and 450

abnormal samples to form the dataset.Some of the sample images from the dataset are shown in Fig. 8. Out of the total database 70% data is used for training and 30% data is used for the testing.

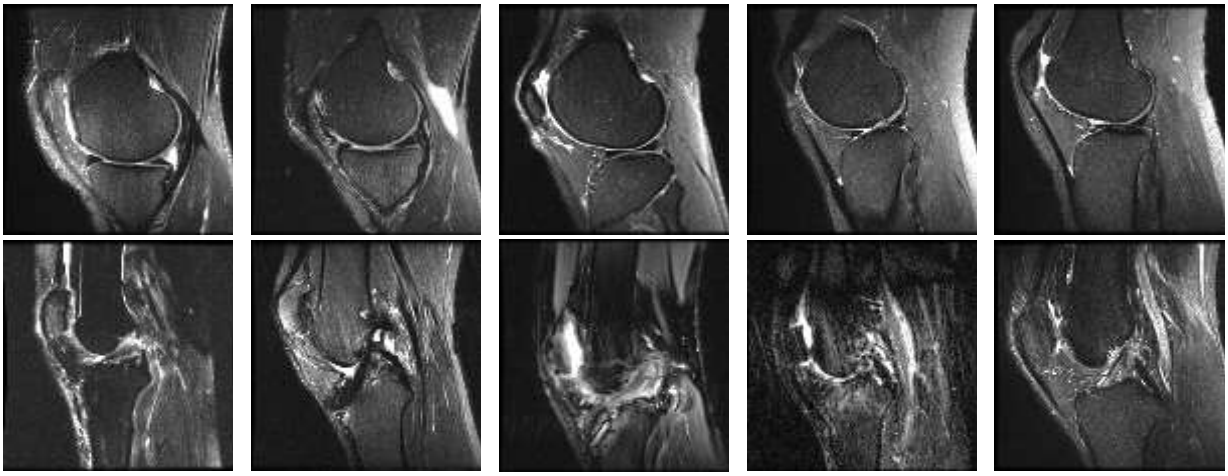

Fig. 8 Sample images from MRNet database

4.2 Discussions on Results

The performance of the proposed algorithm is estimated using accuracy, sensitivity and specificity. Sensitivity gives the measure of correctly identified normal knee ligament samples while specificity describes measure of correctly identified ACL tear samples. The sensitivity, specificity and accuracy for the system is computed using equation 5,6 and 7 where True Positive (TP) represents total number of correctly classified normal knee ligament samples, True Negative (TN) represents total number of correctly classified ACL tear samples, False Negative (FN) represents total number of wrongly classified normal knee ligament samples and False Positive (FP) represents total number of wrongly classified ACL tear samples.

$$\text{Sensitivity} = \frac{\text{TP}}{\text{TP} + \text{FN}} \tag{5}$$

$$\text{Specificity} = \frac{\text{TN}}{\text{TN} + \text{FP}} \tag{6}$$

$$\text{Accuracy}(\%) = \frac{\text{TP} + \text{TN}}{\text{TP} + \text{TN} + \text{FP} + \text{FN}} \times 100 \tag{7}$$

Table I. Performance evaluation of proposed algorithm

Algorithm	Sensitivity	Specificity	Accuracy (%)
LBP+KNN	0.82	0.81	81.70
LBP+SVM	0.83	0.84	83.51
MNLBP+KNN (R=2)	0.83	0.86	84.02
MNLBP+KNN (R=3)	0.87	0.92	88.92
MNLBP+KNN (R=4)	0.80	0.76	78.61
MNLBP+SVM (R=2)	0.85	0.87	86.08
MNLBP+SVM (R=3)	0.88	0.92	89.41
MNLBP+SVM (R=4)	0.81	0.79	80.41

Performance of MNLBP for KNN and SVM classifier is compared with the traditional LBP on the basis of sensitivity, specificity and accuracy as shown in the Table I. the proposed algorithm shows significant improvement over the

LBP. Increasing the radius of the local window increases the performance of the algorithm but larger window (R=4) results in lower performance because of detachment of reference pixels and larger geometrical variations of the texture.

The outcomes of the proposed approach are compared with previous state of arts as described in Table II. It is observed that the proposed approach provided superior compared with existing state of arts that used MRNet dataset for the experimental evaluation. The performance is compared with machine learning schemes utilized for the ACL tear detection.

Table II. Performance comparison of MNLBP with existing machine learning based ACL tear detection

Author and Year	Method	Accuracy
Bienet al. (2018) [17]	AlexNet	81.40%
Kara et al. (2021) [21]	ResNet50	81.27% (Sagittal view)
Proposed Method	MNLBP-SVM	89.41%

It is observed that the proposed method outperforms the existing transfer learning method given by Bien et al. (81.40%) and Kara et al. (81.27%). However, the deep learning techniques require huge number of trainable parameters and add the computational burden on the system. In this case, proposed MNLBP along with SVM provides better results for ACL tear detection for smaller dataset. The selection of the specific volume from the MRI is challenging because of the availability of a large number of volumes in the MRI data.

V. CONCLUSIONS

Thus, this paper presents the ACL tear detection using proposed multi neighbor local binary pattern (MNLBP). Proposed MNLBP can capture the soft texture changes and representation of the geometrical structure of the local region of knee MRI image. It is observed that MNLBP performs better than traditional LBP. The proposed method resulted in sensitivity of 0.87 and 0.88; specificity of 0.92 and 0.92; and accuracy of 88.92% and 89.41% for the KNN and SVM classifiers. Performance of MNLBP is slightly superior for the SVM classifier compared to the KNN classifier.Proposed system detects the presence of ACL tear in the leg MRI and in future it can be extended to the localization of ACL tear in knee MRI. The proposed system provides class imbalance which leads to variation in qualitative and quantitative results of the knee tear detection due to uneven normal and abnormal sample size. In future, effective data augmentation technique can be used to minimize the class imbalance issue.

REFERENCES

1. Davies, George J., Terry Malone, and Frank H. Bassett III, “Knee examination”, Physical Therapy 60, no. 12 (1980): 1565-1574.
2. Pflug, J. J., and J. S. Calnan, “The normal anatomy of the lymphatic system in the human leg”, British Journal of Surgery 58, no. 12 (1971): 925-930.
3. Fukunaga, T., R. R. Roy, F. G. Shellock, J. A. Hodgson, M. K. Day, P. L. Lee, H. Kwong-Fu, and V. R. Edgerton, “Physiological cross-sectional area of human leg muscles based on magnetic resonance imaging”, Journal of orthopaedic research 10, no. 6 (1992): 926-934.
4. Olinski, M., A. Gronowicz, A. Handke, and M. Ceccarelli, “Design and characterization of a novel knee articulation mechanism”, International Journal of Applied Mechanics and Engineering 21, no. 3 (2016): 611-622.
5. https://orthoinfo.aaos.org/en/diseases--conditions/anterior-cruciate-ligament-aclinjuries, Retrieved on 16 Oct 2020.
6. Umap, Rajesh, Bijpuriya Anurag, SachinBagale, and NavidShattari, “Evaluation of Traumatic Knee Joint Injuries with MRI”, International Journal of Contemporary Medicine Surgery and Radiology: 78-81.
7. Andrew Chung, “Knee anatomy, Function and Common Problems”, Healthpages.org, March 30, 2019
8. Ferretti, Andrea, Paola Papandrea, Fabio Conteduca, and Pier Paolo Mariani, “Knee ligament injuries in volleyball players”, The American journal of sports medicine 20, no. 2 (1992): 203-207.

9. Naraghi, Ali M., and Lawrence M. White, "Imaging of athletic injuries of knee ligaments and menisci: sports imaging series", Radiology 281, no. 1 (2016): 23-40.
10. https://www.fda.gov/radiation-emitting-products/medical-imaging/medical-x-ray-imaging. Retrieved on 16 Oct 2020.
11. Grubor, Predrag, Amina Asotic, Milan Grubor, and MithatAsotic, "Validity of magnetic resonance imaging in knee injuries", Acta Informatica Medica 21, no. 3 (2013): 200.
12. ZaheraNaseem, Prof. M. Nasiruddin, "A Review on Analysis of Knee Ligament in Medical Image Processing using Matlab", International Journal of Emerging Technologies and Innovative Research (www.jetir.org), ISSN:2349-5162, Vol.5, Issue 10, page no.641-647, October-2018
13. Stajduhar, Ivan, Mihaela Mamula, Damir Miletic, and Gozde Unal, "Semi-automated detection of anterior cruciate ligament injury from MRI", Computer methods and programs in biomedicine 140 (2017): 151-164.
14. Kohut, Piotr, Krzysztof Holak, and Rafał Obuchowicz, "Image processing in detection of knee joints injuries based on MRI images", Journal of Vibro engineering 19, no. 5 (2017): 3822-3831.
15. Zarychta, Piotr, "Feature vectors of the cruciate ligaments of the knee joint", in 2015 22nd International Conference Mixed Design of Integrated Circuits & Systems (MIXDES), pp. 88-92. IEEE, 2015.
16. Mazlan, S. Syafiq, M. Z. Ayob, and ZA KadirBakti, "Anterior cruciate ligament (ACL) injury classification system using support vector machine (SVM)", in 2017 International Conference on Engineering Technology and Technopreneurship (ICE2T), pp. 1-5. IEEE, 2017.
17. Bien, Nicholas, Pranav Rajpurkar, Robyn L. Ball, Jeremy Irvin, Allison Park, Erik Jones, Michael Bereket et al, "Deep-learning-assisted diagnosis for knee magnetic resonance imaging: development and retrospective validation of MRNet", PLoS medicine 15, no. 11 (2018): e1002699.
18. Lai, ZhiFei, and HuiFang Deng, "Medical Image Classification Based on Deep Features Extracted by Deep Model and Statistic Feature Fusion with Multilayer Perceptron", Computational intelligence and neuroscience 2018 (2018).
19. Liu, Fang, Bochen Guan, Zhaoye Zhou, Alexey Samsonov, Humberto Rosas, Kevin Lian, Ruchi Sharma et al, "Fully automated diagnosis of anterior cruciate ligament tears on knee MR images by using deep learning", Radiology: Artificial Intelligence 1, no. 3 (2019): 180091.
20. Olmez, Emre, Volkan Akdogan, Murat Korkmaz, and Orhan ER, "Automatic Segmentation of Meniscus in Multispectral MRI Using Regions with Convolutional Neural Network (R-CNN)", Journal of Digital Imaging (2020).
21. Kara, Ali Can, and Fırat Hardalaç, "Detection and classification of knee injuries from MR images using the MRNet dataset with progressively operating deep learning methods", Machine Learning and Knowledge Extraction 3, no. 4 (2021): 1009-1029.
22. Germann, Christoph, Giuseppe Marbach, Francesco Civardi, Sandro F. Fucentese, Jan Fritz, Reto Sutter, Christian WA Pfirrmann, and Benjamin Fritz, "Deep Convolutional Neural Network–Based Diagnosis of Anterior Cruciate Ligament Tears: Performance Comparison of Homogenous Versus Heterogeneous Knee MRI Cohorts With Different Pulse Sequence Protocols and 1.5-T and 3-T Magnetic Field Strengths", Investigative radiology 55, no. 8 (2020): 499.
23. T. Ojala, M. Pietikainen, D. Harwood, "A comparative study of texture measures with classification based on feature distributions", Pattern Recognition, 29 (1) (1996) 51–59.
24. Bhangale, Kishor B., and K. Mohanaprasad, "Content Based Image Retrieval using Collaborative Color, Texture and Shape Features", International Journal of Innovative Technology and Exploring Engineering (IJITEE), Volume-9 Issue-3, 2020, pp. 1466-1469.
25. M. Heikkilä, M. Pietikäinen, "A texture-based method for modeling the background and detecting moving objects", IEEE Transactions on Pattern Analysis and Machine Intelligence, 28(4):657-662, 2006.
26. T. Ojala, M. Pietikainen, T. Maenpaa, 'Multiresolution gray-scale and rotation invariant texture classification with local binary patterns", IEEE Trans. Pattern Anal. Mach. Intell. 24 (7) (2002) 971–987.
27. G. Zhao, M. Pietikainen, "Dynamic texture recognition using local binary patterns with an application to facial expressions", IEEE Trans. Pattern Anal. Mach. Intell. 29 (6) (2007) 915–928.
28. A. Hafiane, G. Seetharam, B. Zavidovique, "Median binary pattern for texture classification", in: Proceedings of International Conference on Image Analysis and Recognition, 2007, pp. 387–398.
29. X. Tan, B. Triggs, "Enhanced local texture feature sets for face recognition under difficult lighting conditions", IEEE Trans. Image Process. 19 (6) (2010) 1635–1650.
30. Z. Guo, L. Zhang, D. Zhang, "A completed modeling of local binary pattern operator for texture classification", IEEE Trans. Image Process. 19 (2010) 1657–1663.
31. M. Heikkila, M. Pietikainen, C. Schmid, "Description of interest regions with local binary patterns', Pattern Recognition. 42 (3) (2009) 425–436.
32. B. Zhang, Y. Gao, S. Zhao, J. Liu, "Local derivative pattern versus local binary pattern: face recognition with high-order local pattern descriptor", IEEE Trans. Image Process. 19 (2) (2010) 533–544.
33. Trefny, Jiri, and JiriMatas, "Extended set of local binary patterns for rapid object detection", Proceedings of the Computer Vision Winter Workshop. Vol. 2010. 2010.
34. Z. Guo, Q. Li, J. You, D. Zhang, W. Liu, "Local directional derivative pattern for rotation invariant texture classification", Neural Comput. Appl. 8 (21) (2012) 1893–1904.
35. S. ul Hussain, B. Triggs, "Visual recognition using local quantized patterns", in: Proceedings of European Conference on Computer Vision, Part II, 2012, pp. 716–729.
36. S. A. Orjuela, J. P. Yanez Puentes, P. Philips, S. Brahnam, L. C. Jain, L. Nanni, A. Lumini "The geometric local texture patterns (GLTP), Local Binary Patterns: New Variants and Applications", Springer, Berlin, Heidelberg, 2013, pp. 85–112.

37. T. Ahonen, M. Pietikäinen, “Soft histograms for local binary patterns”, in: Proceedings of Finnish Signal Processing Symposium, 2007, 4 p.
38. S. Katsigiannis, E. Keramidas, D. Maroulis, S. Brahnam, L. C. Jain, L. Nanni, A. Lumini “FLBP: fuzzy local binary patterns, Local Binary Patterns: New Variants and Applications”, Springer, Berlin, Heidelberg, 2013, pp. 149–175.
39. Barkanet. al, “Fast High Dimensional Vector Multiplication Face Recognition”, Proceedings of ICCV 2013
40. C. Ding, J. Choi, D. Tao, and L. S. Davis, “Multi-directional multi-level dual-cross patterns for robust face recognition”, IEEE transactions on pattern analysis and machine intelligence, 38(3):518–531, 2016. 2, 5
41. Bhangale, Kishor B., Kamal M. Jadhav, and Yogesh R. Shirke, “Robust Pose Invariant Face Recognition using DCP and LBP”, International Journal of Management, Technology and Engineering 8, no. IX (2018): 1026-1034.
42. Xu, Yong, Qi Zhu, Zizhu Fan, Minna Qiu, Yan Chen, and Hong Liu, “Coarse to fine K nearest neighbor classifier”, Pattern recognition letters 34, no. 9 (2013): 980-986.
43. Bhangale, Kishor B., and R. U. Shekokar, “Human body detection in static images using hog & piecewise linear svm”, International Journal of Innovative Research & Development 3, no. 6 (2014).
44. Dattatraya, K.N., , “Hybrid based cluster head selection for maximizing network lifetime and energy efficiency in WSN”, Journal of King Saud University - Computer and Information Sciences, 2022, 34(3), pp. 716–726
45. Dattatraya, K.N., Raghava Rao, K, “Maximising network lifetime and energy efficiency of wireless sensor network using group search Ant lion with Levy flight”, IET Communications, 2020, 14(6), pp. 914–922.
46. Ramkumar, J., Karthikeyan, C., Vamsidhar, E., Dattatraya, K.N., “Automated pill dispenser application based on IoT for patient medication”, EAI/Springer Innovations in Communication and Computing, 2020, pp. 231–253.
47. Dattatraya, K.N., Raghava Rao, K., Satish Kumar, D., “Architectural analysis for lifetime maximization and energy efficiency in hybridized WSN model”, International Journal of Engineering and Technology(UAE), 2018, 7, pp. 494–501.
48. Dattatraya, K.N., Ananthakumaran, S., “Energy and Trust Efficient Cluster Head Selection in Wireless Sensor Networks Under Meta-Heuristic Model”, Lecture Notes in Networks and Systems, 2022, 444, pp. 715–735.
49. Dattatraya, K.N., Ananthakumaran, S., Kiran, K.V.D., “Optimal cluster head selection in wireless sensor network via improved moth search algorithm”, Artificial Intelligence in Information and Communication Technologies, Healthcare and Education: A Roadmap Ahead, 2022, pp. 95–108.
50. Kishor B. Bhangale “Synthetic Speech Spoofing Detection Using MFCC and SVM.” IOSR Journal of Engineering (IOSRJEN), vol. 08, no. 6, 2018, pp. 55-61.
51. Burduk, Robert, and JedrzejBiedrzycki, “Integration and Selection of Linear SVM Classifiers in Geometric Space”, J. UCS 25, no. 6 (2019): 718-730.
52. https://stanfordmlgroup.github.io/competitions/mrnet/. Retrieved on 8 Aug 2020.